SIMULTANEOUS DESIGN AND OPERATIONAL OPTIMIZATION FOR FLEXIBLE CARBON CAPTURE PLANTS

Kyeongjun Seo, Adhika P. Retnanto, Jorge L. Martorell, Mark A. Stadtherr, Thomas F. Edgar, and Michael Baldea[1]

McKetta Department of Chemical Engineering, The University of Texas at Austin, Austin, TX 78712

Abstract

Carbon capture and sequestration (CCS) is an essential means to mitigate carbon emissions from power plants. Given the increase of energy generation from variable renewable energy (VRE) systems such as solar and wind, conventional power generation systems are likely to operate increasingly at variable generation rates to balance the intermittent power supply from renewable sources. Consequently, carbon capture systems that are (or will be) integrated with fossil-fueled power plants are expected to operate at variable load. In addition, solvent regeneration and compression of CO_2 require large amounts of energy, and increasing the flexibility of carbon capture (specifically, using variable capture rates in conjunction with solvent storage, effectively decoupling solvent regeneration from carbon capture) allows operators to take advantage of fluctuating electricity prices to make up for the cost of CCS systems. Motivated by the above, we analyze the flexibility of carbon capture plants using ionic liquids (ILs) as the solvent. We use a rate-based dynamic model to optimize the overall process cost under real-world scenarios and study the optimal flexible operation of a carbon capture unit in a high VRE adoption environment.

Keywords

Carbon Capture and Sequestration, Variable Renewable Energy, Flexibility, Optimization, Ionic Liquids

Introduction

Fossil-fuel-based power plants contribute a large fraction of the anthropogenic carbon dioxide and other greenhouse gas (GHG) emissions that drive global warming (U.S. Energy Information Administration, 2022; The Intergovernmental Panel on Climate Change, 2018). At the same time, the contribution of renewables to the power generation portfolio is rapidly growing, driven largely by wind and solar photovoltaics (PV). These energy sources are key to reducing greenhouse gas emissions in order to meet climate change mitigation targets. However, their power output fluctuates both during the day and seasonally, creating significant challenges in balancing supply and demand on the power grid.

A well-known example of the impact of increasing the contribution of variable renewable energy (VRE) to the power generation mix is the “duck curve” of the net demand (total demand minus solar PV supply) over the course of a day. Solar PV supply tends to increase rapidly at sunrise, peak at midday, and fall rapidly at sunset. Electricity demand, on the other hand, peaks in the evening as PV supply declines. This results in rapid changes in the net demand which, in the absence of grid-level energy storage, must be met by quickly ramping up output of conventional power plants.

Overall, increasing the adoption of VRE reduces the demand for electricity from (dispatchable) thermal power plants. However, the need for backup capacity when VRE is unavailable means that adding VRE capacity to the grid does not immediately and fully displace conventional generation facilities. Instead, such plants must operate at lower capacity factors with more frequent cycling (Mills et al., 2020). These requirements are driving a need for flexible fossil fuel power plants, having faster dynamics, greater turndown ratios, and better efficiency in off-design operation (Gonzalez-Salazar et al., 2018). Fossil fuel plants, particularly using natural gas combined cycle (NGCC) technology, are in fact projected to provide a not-insignificant share of US electricity generation (U.S. Energy Information Administration, 2022) well into the middle of this century. Carbon capture and sequestration (CCS) remains a key component of any strategy for reducing CO_2 emissions from the power sector (IPCC, 2022), and retrofitting existing power plants is essential. Making use of existing generation assets provides capital savings, and provides an opportunity for continued operations where future cuts in CO_2 emissions might be required (Fan et al., 2018).

The need for flexible operation of power plants must in-

[1] Corresponding author. Email: mbaldea@che.utexas.edu.

form the design and operation of the associated CCS processes. CCS process flexibility is associated with several design features (Cohen et al., 2012; Spitz et al., 2019), including but not limited to, i) the ability to modulate the capture rate over time, while maintaining the overall, time-average capture rate at the target value (at present, it is typical to aim for capturing 90% of the CO_2 present in a stream released to the atmosphere) and ii) the ability to store solvent rich in CO_2 in a tank. The flexibility benefits of these features can be explained as follows:

- Decreasing the capture rate during times of peak power demand allows for reducing the amount of energy (typically, low pressure steam) that is diverted from power generation and used for solvent recovery. This is particularly useful when power demand on the grid is very high. The reduction in capture rate can be compensated by increasing capture rates above the nominal value at times when power demand is low.

- Storing CO_2-rich solvent decouples the energy-intensive solvent regeneration process from carbon capture and the operation of the power plant. This expands the range of net power plant output by allowing a lower minimum output when prioritizing solvent regeneration during periods of low net demand and a higher maximum output during peak demand periods.

Ultimately, the flexibility of the CCS system allows a power plant to perform price arbitrage (Cohen et al., 2012), i.e., generating power during peak demand periods, when electricity prices are high, and performing solvent regeneration/make-up capture when grid demand is low (Mills et al., 2020). This can lead to increased revenue that can compensate for the high cost of installing the CCS facility. Additional benefits could in principle be derived from exploiting incentives such as carbon taxes, carbon credits, etc.

Motivated by the above, in this work, we consider an ionic-liquid-based carbon capture system with the aforementioned flexibility-enhancing features (solvent storage and variable capture level). Recently, ionic liquids (ILs) have been studied as a promising class of carbon capture solvents that provides superior properties such as lower heats of absorption and negligible volatility, relative to established aqueous amine solvents (Aghaie et al., 2018). We first present a dynamic CO_2 capture process flowsheet model, and subsequently formulate and solve a scenario-based optimization problem that identifies the optimal design and strategy operation for implementing this process for capturing CO_2 from the flue gas of an NGCC power plant operating in highly dynamic electricity markets.

CO_2 Capture Process Model

The IL-based CO_2 capture flowsheet model is based on the steady-state flowsheet model developed by Seo et al. (2020) with some modifications. Figure 1 illustrates an IL-based carbon capture process. The process consists of an absorber and a solvent regeneration section represented as a flash separator. The CO_2 in the flue gas is absorbed by IL in the packed-bed absorption column. To enhance the absorption efficiency, a solvent intercooling system is utilized. The CO_2-rich solvent leaves the absorber at the bottom and is preheated in a feed-effluent heat exchanger using the hot CO_2-lean (regenerated) solvent. The CO_2-rich solvent is then regenerated using a heated flash and recycled back to the absorber, while the captured CO_2 is compressed for storage or further use. In this system, solvent regeneration can be delayed during peak electricity demand/prices by storing the rich solvent in a tank. In addition, the CO_2 capture level can be reduced selectively for a period of time reducing energy consumption for solvent regeneration and CO_2 compression. Alternatively, lean solvent from the lean solvent tank is available to increase capture rates when desired, again without necessarily increasing energy use for regeneration at that time.

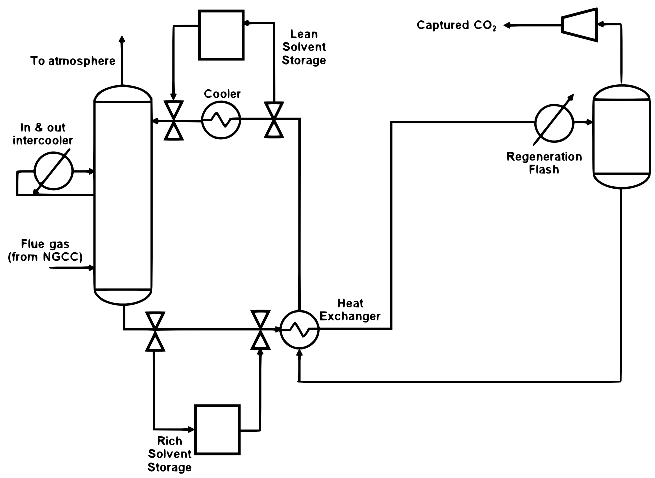

Figure 1: IL-based carbon capture process flowsheet

In this work, we consider the IL solvent triethyl-(octyl)phosphonium 2-cyanopyrrolide ($[P_{2228}]$[2-CNPyr]) due to its high absorption capacity, moderate reaction enthalpy, superior reversibility, and relatively low viscosity (Seo et al., 2014). CO_2 absorption is described by the equilibrium uptake model proposed by Hong et al. (2016) in which the overall absorption is represented as the sum of physical and chemical absorption:

$$X = X_{\text{phys}} + X_{\text{chem}} = \frac{P_{CO_2}}{H(T)} + \frac{K_{\text{eq}}(T)P_{CO_2}C_3(T)}{1+K_{\text{eq}}(T)P_{CO_2}} \quad (1)$$

where X_{phys} and X_{chem} represent, respectively, the physical and chemical uptake of CO_2 by the IL (mol CO_2 /mol IL). $H(T)$ is the Henry's constant and P_{CO_2} is the CO_2 partial pressure. K_{eq} is the chemical absorption equilibrium constant and $C_3(T)$ refers to a factor for the reaction site density.

One of the most important considerations in the flowsheet model is kinetically limited gas mass transfer in the absorption column. The relevant material balances for the vapor and liquid phases in the absorption column can be expressed as:

$$\frac{1}{LS}\frac{\partial\left(F^{\mathrm{V}}y_i\right)}{\partial z} = -N_i^{\mathrm{V}}, \quad i = \mathrm{CO_2}, \mathrm{N_2}, \mathrm{O_2} \tag{2}$$

$$\sum y_i = 1, \quad i = \mathrm{CO_2}, \mathrm{N_2}, \mathrm{O_2} \tag{3}$$

$$\frac{\partial\left(\varepsilon_{\mathrm{L}}C_i^{\mathrm{L}}\right)}{\partial t} + \frac{1}{LS}\frac{\partial\left(F^{\mathrm{L}}x_i\right)}{\partial z} = N_i^{\mathrm{L}}, \quad i = \mathrm{CO_2}, \mathrm{IL} \tag{4}$$

$$\sum x_i = 1, \quad i = \mathrm{CO_2}, \mathrm{IL} \tag{5}$$

where z is the normalized axial position and L and S are the height and cross-sectional area of the column, respectively. F^{V} and F^{L} are the vapor and liquid molar flowrates, and y_i and x_i represent the vapor and liquid phase mole fractions for component i. ε_{L} is the liquid hold-up in the packing and C_i^{L} is the molar density for the component i. Note that molar hold-up in the vapor phase is much smaller than that in the liquid phase, therefore, the vapor phase dynamics are assumed to be negligible (Walters et al., 2016a). N_i refers to the molar transfer rates (per unit volume of bed) of each component i and can be expressed by:

$$N_i^{\mathrm{L}} = N_i^{\mathrm{V}} = a_{\mathrm{e}}K_{\mathrm{g},i}(P_i - P_i^*) \tag{6}$$

$$\frac{1}{K_{\mathrm{g},i}} = \frac{1}{k_{\mathrm{g},i}} + \frac{1}{E_{0,i}k_{\mathrm{l},i}} \tag{7}$$

where P_i is the partial pressure of component i in the vapor phase, P_i^* is the equilibrium pressure of gas component i in the liquid phase, and a_{e} is the effective area of packing. $K_{\mathrm{g},i}$ is the overall mass transfer coefficient and can be calculated based on gas and liquid phase mass transfer resistance, $k_{\mathrm{g},i}$ and $k_{\mathrm{l},i}$, and an enhancement factor, $E_{0,i}$, which quantifies the increased mass transfer rate due to chemical reaction between CO_2 and IL. Further details on these models are presented by Seo et al. (2020, 2021).

In order to model process dynamics, we assume first-order responses for the process components that feature significant material holdup (Walters et al., 2016b). Specifically, we assume residence times in the absorber sump and flash tank are $\tau = 5$ min. Thus, for these units, we model concentrations and enthalpies as:

$$\tau\frac{\partial\chi_{\mathrm{out}}}{\partial t} = \chi_{\mathrm{in}} - \chi_{\mathrm{out}} \tag{8}$$

where χ_{in} and χ_{out} are the relevant inlet and outlet properties.

Flexible Operation of CO_2 Plant

Figure 2 shows the impact of fluctuating energy prices on the operation of a natural gas combined cycle (NGCC) power plant. We use day-ahead electricity market prices in Texas (Electric Reliability Council of Texas, 2022) and Wolf Hollow II power station (located in Granbury, Texas) output data (United States Environmental Protection Agency, 2022a). Texas was selected as a location given that wind and solar account for over 20% of the electricity generation at the level of the local independent system operator (ERCOT) (United States Environmental Protection Agency, 2022b), thereby influencing electricity prices significantly. We chose three example days in 2020 that represent high, moderate, and low fluctuations in electricity prices. The power plant output varies between 300 and 1100 MW on a daily basis in response to the grid demand. We assume that the feed composition of flue gas is constant with that reported in DOE baseline case B31B (NGCC plant with a net output of 646 MW) (James et al., 2019).

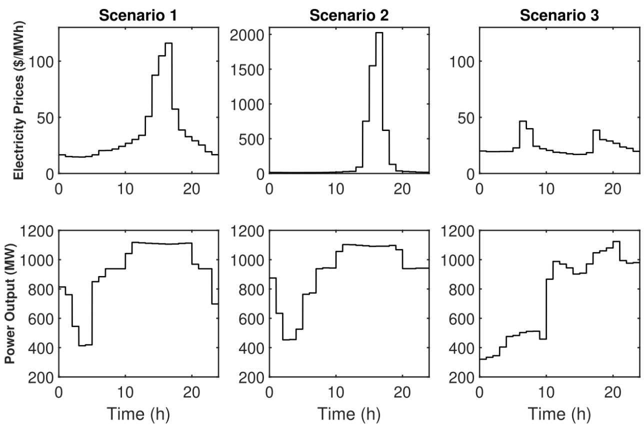

Figure 2: Day ahead electricity prices and power output of the NGCC power station. Case 1: moderate, Case 2: high, Case 3: low fluctuations in electricity market prices

Considering this impact of changing energy trends on the power station operation, it is desirable to design and operate the accompanying carbon capture process accordingly. To find the optimal design and operation corresponding to these fluctuations, we solve a scenario-based optimization problem:

$$\begin{aligned} \min_{d,z} \quad & \sum_{k=1}^{3}\left(w_k\int_0^{t_f} f_k\left(d, x_k(t), z_k(t), \theta_k(t)\right)dt\right) \\ \text{s.t.} \quad & \text{carbon capture plant dynamic model} \\ & \text{operating constraints} \end{aligned} \tag{9}$$

where the objective function comprises the scenario-weighted process costs of the IL-based CO_2 capture process for the time horizon considered (24 h in this work). f represents process costs that include capital, operating, and initial solvent start-up costs. Detailed cost correlation models are available in our previous work (Seo et al., 2020). k refers to the three scenarios considered (high, moderate, low variations). w_k represents scenario weights, which are probabilities of each scenario in a long term operation (weights for high, moderate, and low cases are 0.0082, 0.3224, and 0.6694, respectively, considering ERCOT electricity price data in 2020). d and z are, respectively, the process design variables (e.g., sizes of unit operations) and the operating variables (e.g., flowrate, temperature) being optimized. Note that the process design does not change depending on the scenario. x_k are process variables and θ_k are time-varying parameters that represent fluctuations in energy prices and flue gas load. Operating constraints include an overall time-average CO_2 removal of at least 90%, and a minimum heat exchanger approach temperature of 1 °C. Additionally, solvent cannot flow in and out of a storage tank at the same time, and the inventory levels in the lean and rich solvent storage tanks must return to the initial values at the end of

Table 1: Optimal values of key process design and operation variables

Decision variables	Inflexible	Flexible	Lower bound	Upper bound
Absorber height (m)	7.53	7.44	1	20
Absorber diameter (m)	22.8	25.9	1	20
Rich solvent storage max inlet flowrate [$k = 1$] (kmol/s)	-	0.86	0	10
Rich solvent storage max inlet flowrate [$k = 2$] (kmol/s)	-	1.20	0	10
Rich solvent storage max inlet flowrate [$k = 3$] (kmol/s)	-	0.45	0	10
Lean solvent storage max outlet flowrate [$k = 1$] (kmol/s)	-	0.84	0	10
Lean solvent storage max outlet flowrate [$k = 2$] (kmol/s)	-	1.57	0	10
Lean solvent storage max outlet flowrate [$k = 3$] (kmol/s)	-	0.37	0	10
Rich solvent storage capacity (m^3)	-	26,813	0	50,000
Lean solvent storage capacity (m^3)	-	23,332	0	50,000

the time horizon. Inventory levels are constrained to be from 20% to 80% of the storage tank volume. The resulting model has 6075 equations and the optimization problem is solved in gPROMS ProcessBuilder using the NLPSQP solver. The optimization problem is solved within 15 hours of CPU time on a 64 bit Windows 10 PC with an Intel Core i7, 3.20 GHz processor and 16.0 GB RAM.

Table 1 shows the optimal values of key design and operation variables for the carbon capture system considered in this work. Comparison is also made to optimal values for a case without flexibility (i.e., the same problem but with constant capture rate and no solvent storage capabilities). The optimal diameter for the packed volume of the absorber column is larger in the flexible operation to accommodate the increased liquid flowrates made possible by the storage system. Solvent inlet/outlet flowrates from storage decrease as the degree of fluctuation in electricity market price decreases. With the lowest level of fluctuation (case 3), the overall carbon capture rate target can be met largely by modulating process operating variables to adjust the instantaneous capture level, thus making use of solvent storage less important. Operating without storage tanks would be practical for such low-price variation situations, but storage tanks are needed in the overall optimal design when low, medium and high price variability scenarios must all be considered.

Figure 3 shows the optimal CO_2 capture and rich storage levels as a function of time for each scenario. The initial rich storage levels (different for each scenario) were set to provide one hour of solvent flow, assuming a solvent flow rate equal to the optimal solvent flow rate for that scenario in the case without flexibility, and respecting the constraint that the level cannot fall below 20% of nominal full capacity. The overall CO_2 capture level over 24 hours of operation is 90% in all cases. The instantaneous CO_2 capture levels shown in Figure 3 are calculated as the ratio of the captured CO_2 flow rate to the total CO_2 flow rate in the flue gas. With this definition, it is possible for the instantaneous capture level to exceed 100% due to system dynamics or consumption of rich and lean solvent inventory. The capture rate is minimized during the peak electricity price hours of $t = 14$ to 16 h for the moderate (case 1) and high (case 2) price variation cases and $t = 6$ to 8 h for the low variation case, and increases during periods of lower electricity cost to compensate. As already noted in discussing Table 1, there is relatively little usage of the storage capacity in the low variation scenario (case 3). In the moderate and high variation scenarios (cases 1 and 2, respectively), the CO_2-rich solvent is sent to storage during peak electricity price hours.

The optimized annualized capital cost for the flexible operation is 3.8% higher compared to the case without flexibility (no solvent storage tanks, constant capture rate). This is primarily due to increased costs in the flexible case for a larger absorber and heat exchanger, and the introduction of the storage system. However, the results show a 5.8% savings in the overall process cost (objective function f in eqn (9)) for a 24 h operating period compared to the case without flexibility. This can be mainly attributed to the avoidance of regeneration and compression during periods of high electricity prices.

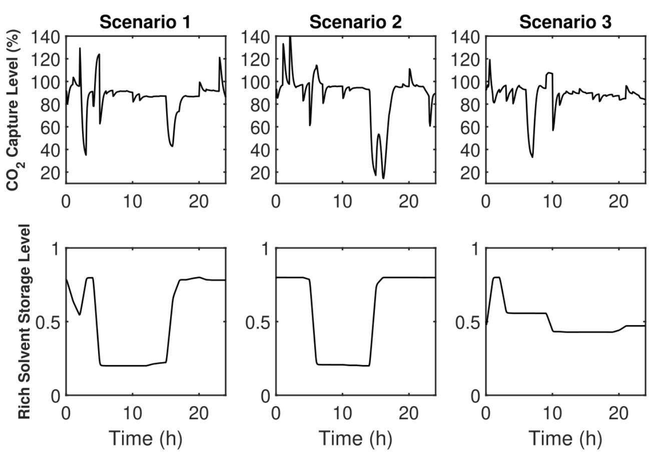

Figure 3: Optimized CO_2 capture level (top) and rich solvent storage level (bottom)

Conclusions

With increasing penetration of VRE, power plants must be able to undergo frequent load changes in response to variations in overall energy demand and VRE supply. Flexible operation of carbon capture plants can mitigate the large electricity cost penalties for carbon capture that could arise due to such fluctuations.

In this work, we present an IL-based dynamic CO_2 capture plant model with consideration of mass transfer limitation during CO_2 absorption. Solvent storage and variable carbon capture rate are introduced to enable flexible operation. We present a scenario-based optimization framework for a carbon capture process connected to an NGCC power plant. The results provide optimal design and operating conditions in response to fluctuations in load and electricity prices. Flexible operation is found to provide important economic savings.

Acknowledgments

The authors gratefully acknowledge the financial support provided by ExxonMobil through the Fueling a Sustainable Energy Transition (FSET) program of the University of Texas at Austin Energy Institute. KS was partially supported by the Phillips 66 Fellowship and the Graduate School Fellowship at the University of Texas. Partial financial support from the National Science Foundation under the ECO CBET award 2133543 is also acknowledged.

References

Aghaie, M., N. Rezaei, and S. Zendehboudi (2018). A systematic review on CO_2 capture with ionic liquids: Current status and future prospects. *Renewable Sustainable Energy Rev. 96*, 502–525.

Cohen, S. M., M. E. Webber, and G. T. Rochelle (2012). The impact of electricity market conditions on the value of flexible CO_2 capture. In *ASME 2012 Int. Mech. Eng. Congress and Exposition*, Volume 6: Energy, Parts A and B, pp. 581–593.

Electric Reliability Council of Texas (2022). Day-ahead price. `http://www.ercot.com/`.

Fan, J.-L., M. Xu, F. Li, L. Yang, and X. Zhang (2018). Carbon capture and storage (CCS) retrofit potential of coal-fired power plants in China: The technology lock-in and cost optimization perspective. *Applied Energy 229*, 326–334.

Gonzalez-Salazar, M. A., T. Kirsten, and L. Prchlik (2018). Review of the operational flexibility and emissions of gas- and coal-fired power plants in a future with growing renewables. *Renewable Sustainable Energy Rev. 82*, 1497–1513.

Hong, B., L. D. Simoni, J. E. Bennett, J. F. Brennecke, and M. A. Stadtherr (2016). Simultaneous process and material design for aprotic *N*-heterocyclic anion ionic liquids in postcombustion CO_2 capture. *Ind. Eng. Chem. Res. 55*, 8432–8449.

IPCC (2022). Energy Systems. In *Climate Change 2022: Mitigation of Climate Change. Contribution of Working Group III to the Sixth Assessment Report of the Intergovernmental Panel on Climate Change*, Chapter 6, pp. 6-1 – 6-183. Cambridge, UK and New York, NY, USA: Cambridge University Press.

James, R. E., D. Kearins, M. Turner, M. Woods, N. Kuehn, and A. Zoelle (2019). Cost and Performance Baseline for Fossil Energy Plants Volume 1: Bituminous Coal and Natural Gas to Electricity. Technical Report NETL-PUB-22638, U.S. Department of Energy.

Mills, A. D., T. Levin, R. Wiser, J. Seel, and A. Botterud (2020). Impacts of variable renewable energy on wholesale markets and generating assets in the United States: A review of expectations and evidence. *Renewable Sustainable Energy Rev. 120*, 109670.

Seo, K., Z. Chen, T. F. Edgar, J. F. Brennecke, M. A. Stadtherr, and M. Baldea (2021). Modeling and optimization of ionic liquid-based carbon capture process using a thin-film unit. *Comput. Chem. Eng. 155*, 107522.

Seo, K., C. Tsay, B. Hong, T. F. Edgar, M. A. Stadtherr, and M. Baldea (2020). Rate-based process optimization and sensitivity analysis for ionic-liquid-based post-combustion carbon capture. *ACS Sustainable Chem. Eng. 8*, 10242–10258.

Seo, S., M. Quiroz-Guzman, M. A. DeSilva, T. B. Lee, Y. Huang, B. F. Goodrich, W. F. Schneider, and J. F. Brennecke (2014). Chemically tunable ionic liquids with aprotic heterocyclic anion (AHA) for CO_2 capture. *J. Phys. Chem. B 118*(21), 5740–5751.

Spitz, T., A. González Díaz, H. Chalmers, and M. Lucquiaud (2019). Operating flexibility of natural gas combined cycle power plant integrated with post-combustion capture. *Int. J. Greenh. Gas Con. 88*, 92–108.

The Intergovernmental Panel on Climate Change (2018). Global warming of 1.5 C. `https://www.ipcc.ch/sr15/`.

United States Environmental Protection Agency (2022a). Air markets program data. `https://ampd.epa.gov/ampd/`.

United States Environmental Protection Agency (2022b). State electricity profiles. `https://www.eia.gov/electricity/state/texas/`.

U.S. Energy Information Administration (2022). Annual energy outlook 2022. `https://www.eia.gov/outlooks/aeo/`.

Walters, M. S., T. F. Edgar, and G. T. Rochelle (2016a). Dynamic modeling and control of an intercooled absorber for post-combustion CO_2 capture. *Chem. Eng. Process. 107*, 1–10.

Walters, M. S., T. F. Edgar, and G. T. Rochelle (2016b). Regulatory control of amine scrubbing for CO_2 capture from power plants. *Ind. Eng. Chem. Res. 55*(16), 4646–4657.